

# Concussive Injury before or after Controlled Cortical Impact Exacerbates Histopathology and Functional Outcome in a Mixed Traumatic Brain Injury Model in Mice

Heda R. Dapul,<sup>1,2</sup> Juyeon Park,<sup>1,2</sup> Jimmy Zhang,<sup>1,2</sup> Christopher Lee,<sup>1,2</sup> Ali DanEshmand,<sup>1,3</sup>  
Josephine Lok,<sup>1,2</sup> Cenk Ayata,<sup>1,3,4</sup> Tory Gray,<sup>2</sup> Allison Scalzo,<sup>5</sup> Jianhua Qiu,<sup>1,2</sup>  
Eng H. Lo,<sup>1,3,4</sup> and Michael J. Whalen<sup>1,2</sup>

## Abstract

Traumatic brain injury (TBI) may involve diverse injury mechanisms (e.g., focal impact vs. diffuse impact loading). Putative therapies developed in TBI models featuring a single injury mechanism may fail in clinical trials if the model does not fully replicate multiple injury subtypes, which may occur concomitantly in a given patient. We report development and characterization of a mixed contusion/concussion TBI model in mice using controlled cortical impact (CCI; 0.6 mm depth, 6 m/sec) and a closed head injury (CHI) model at one of two levels of injury (53 vs. 83 g weight drop from 66 in). Compared with CCI or CHI alone, sequential CCI-CHI produced additive effects on loss of consciousness ( $p < 0.001$ ), acute cell death ( $p < 0.05$ ), and 12-day lesion size ( $p < 0.05$ ) but not brain edema or 48-h contusion volume. Additive effects of CHI and CCI on post-injury motor ( $p < 0.05$ ) and cognitive ( $p < 0.005$ ) impairment were observed with sequential CCI-CHI (83 g). The data suggest that concussive forces, which in isolation do not induce histopathological damage, exacerbate histopathology and functional outcome after cerebral contusion. Sequential CHI-CCI may model complex injury mechanisms that occur in some patients with TBI and may prove useful for testing putative therapies.

**Key words:** brain injury; cognition; concussion; controlled cortical impact; mice; models

## Introduction

**I**N 2007, the National Institute of Neurological Disorders and Stroke sponsored a workshop entitled Classification of Traumatic Brain Injury (TBI) for Targeted Therapies.<sup>1</sup> The committee recognized that development of rational therapeutic strategies for TBI might be facilitated by a classification scheme based on mechanism of injury (e.g., focal impact loading producing contusions, diffuse impact loading producing concussion, inertial loading producing diffuse axonal injury/subdural hematoma, etc.).<sup>1,2</sup> The committee also recognized that multiple injury mechanisms (e.g., concussion and contusion) could occur in a given patient, leading to heterogeneity of injury subtypes that might complicate development of therapeutic strategies if the targeted pathophysiological mechanism(s) were differentially regulated in one injury subtype versus another. A limitation of most rodent and large animal TBI models is that they incorporate one predominant brain injury subtype and may therefore fail to account for injury heterogeneity in TBI patients. This shortcoming may contribute to treatment failure in clinical trials for TBI.<sup>3</sup>

Controlled cortical impact (CCI) has been widely used to model cerebral contusion in mice.<sup>4–8</sup> Because the head is held fixed in a stereotaxic frame, CCI does not impart acceleration/deceleration forces characteristic of concussive TBI, which is characterized by linear or angular acceleration of the head.<sup>9–11</sup> We recently published a closed head injury (CHI) model of concussive TBI in mice in which the head freely rotates in the anterior-posterior plane.<sup>12</sup> The CHI model is distinct from CCI inasmuch as it produces cognitive deficits in the absence of contusion, acute cell death, edema, significant axonal injury, or chronic brain tissue loss.

Because no experimental TBI study has examined concussive and contusion injury mechanisms separately and together, it remains unknown how the presence of both injury subtypes might influence outcome. This is an important gap in the literature for at least two reasons. First, similar cellular and biochemical mechanisms may differentially affect outcome in contusion and concussion, making assessment of molecular therapeutic targets for patients with both injury subtypes problematic.<sup>5,12</sup> Second, treatments that work in one injury subtype may be ineffective or even detrimental in another, leading to treatment failure in the scenario

<sup>1</sup>Neuroscience Center, Departments of <sup>2</sup>Pediatric Critical Care Medicine, <sup>3</sup>Radiology, <sup>4</sup>Neurology, Massachusetts General Hospital, Harvard Medical School, Charlestown, Massachusetts.

<sup>5</sup>Pennsylvania State University, University Park, Pennsylvania.

in which two (or more) injury subtypes coexist. To begin to address this knowledge gap, we developed a new model of sequential CCI-CHI in mice and examined the effect of both injury subtypes on clinically relevant outcome measures, including loss of consciousness, brain edema, lesion size, and motor and cognitive function.

## Methods

### Animals

Mice were housed for 12-h day/night cycles in a pathogen-free facility at Massachusetts General Hospital Institutional Animal Care in accordance with the National Institutes of Health Guide for Care and Use of Laboratory Animals. Food and water were given *ad libitum*. Adult C57/BL6 male mice (8–16 weeks of age; Jackson Laboratories, Bar Harbor, ME) were used. All trauma protocols were approved by the Massachusetts General Hospital Institutional Animal Care and Use Committee.

### CCI

The CCI model was used as previously described.<sup>13</sup> Anesthesia was induced using a Fluotec 3 vaporizer (Colonial Medical, Amherst, NH) and 70% nitrous oxide, 4–5% isoflurane (Anaquest, Memphis, TN), and balance oxygen. After induction, mice were removed from the chamber, positioned on a stereotaxic frame with the nose placed in an opening of a plastic tubing carrying anesthesia from the chamber to the animal and then out into a negative pressure hood. Isoflurane was reduced to 3.5–4%. Side stream ventilation of room air mixed with isoflurane produces unresponsiveness to tail and toe pinch and to surgical procedures, yet maintains blood pressure and blood gases within normal limits in CHI and CCI models.<sup>13–15</sup>

A 5-mm craniotomy was made with a portable drill and trephine over the left parietotemporal cortex. The bone flap was removed, and the dura was left intact. Impact was delivered using a 3-mm flat-tip pneumatic piston at a velocity of 6 m/sec, duration 100 ms, and depth of 0.6 mm. The bone flap was discarded and the scalp incision sutured closed. Sham-injured mice underwent craniotomy but not CCI. Loss of consciousness (LOC) time was the time between removal from anesthesia to spontaneous ambulation.

### CHI

CHI was administered using a modification of a recently published protocol.<sup>12</sup> Isoflurane anesthesia was given for 45 seconds, then CHI was performed by placing the mouse on a Kimwipe (Kimberly-Clark, Irving, TX) with its head positioned under a hollow tube (66" length, 10 mm diameter), right ear facing upward. A metal bolt (53 or 83 g) was dropped through the tube and impacted the head behind the right ear, thus avoiding the craniotomy site from CCI in sequential injury mice, and allowing the head to freely rotate downward into the Kimwipe. LOC time was measured from time of impact to spontaneous ambulation.

### Sequential head injury

A combination of contusion and concussion injury was performed using either CCI followed by CHI (CCI-CHI) or CHI followed by CCI (CHI-CCI). The time period between the two injuries was 1–2 minutes. In the CCI-CHI model, mice were subjected to a total of 4 min of 4% isoflurane anesthesia. Mice were placed on a stereotaxic frame where CCI was performed. The scalp was quickly sutured closed and the animal removed from the frame and subjected to CHI. For CCI-CHI, LOC time was measured from time of CHI impact to spontaneous ambulation. In the CHI-CCI model, animals again received a total of approximately 4 min of anesthesia. After anesthesia induction, CHI was performed, and mice were rapidly placed in a stereotaxic frame and subjected to

CCI. For CHI-CCI, LOC time was measured from the time of removal from anesthesia to spontaneous ambulation.

### Assessment of post-traumatic seizure activity

Mice were observed for seizure activity during LOC time and while awake in the immediate post-injury period. Criteria for behavioral seizures included any of the following: arrest of motion, myoclonic jerks of the head and neck, brief twitching movements of forelimbs and hindlimbs, bilateral tonic-clonic forelimb or hindlimb activity, or generalized tonic-clonic activity with rearing and loss of postural tone.<sup>16,17</sup> Mice classified as having no seizure activity lacked any of the aforementioned behavioral manifestations. Seizure activity was scored by the same operators who performed trauma.

### Physiological variables

Mice ( $n = 5$ ) were anesthetized and the femoral artery cannulated with P10 tubing (Intramedic polyethylene tubing P10, Becton-Dickenson, Franklin Lakes, NJ). Arterial blood gases were drawn at 1 and 5 min post-injury. Blood pressure was monitored continuously for 1–5 min after sequential injury (Power Lab, AD Instruments, Colorado Springs, MO).

### Assessment of vestibular-motor function

Vestibular-motor function was assessed between 1–7 days post-injury using the wire-grip test.<sup>5</sup> Mice were placed on a wire 45 cm in length, suspended 45 cm above a padded surface. The length of time they remained on the wire within a 60 sec interval was measured, as well as their wire grip score, which was quantified using a 5-point scale. An average of 3 trials was calculated for each mouse on each test day.

### Morris water maze

The Morris water maze (MWM) was used to evaluate spatial learning and memory beginning 7–10 days after injury to allow for recovery of motor deficits.<sup>5</sup> The apparatus consisted of a white pool 83 cm in diameter and 60 cm deep, filled with water to a depth of 29 cm. Visible cues were positioned on the walls of the tank and around the room. Water temperature was maintained approximately 25°C. A clear Plexiglas goal platform 10 cm in diameter was positioned 0.5 cm below the surface of the water (hidden platform), approximately 15 cm from the southwest wall (target quadrant) of the tank.

Each mouse was subjected to two trials per day. After five sets of hidden platform trials and one probe trial, two sets of visible platform trials were performed. For each trial, mice were randomized to one of four starting locations (North, South, East and West) and placed in the pool facing the wall. The maximum time allotted to reach the platform was 90 sec. If the mouse failed to reach the platform within the allotted time, it was placed on the platform by the experimenter and allowed to remain there for 10 sec. In the probe trial, the goal platform was removed, mice were placed in the tank opposite the target quadrant, and the time spent in the target quadrant was assessed over 60 sec. The probe score was time in seconds spent by the mouse in the target quadrant. Visible platform trials were performed on the day after the probe trial. For the visible trials, the goal platform was raised 0.5 cm above the water and clearly marked with red tape (visible platform). Performance in the hidden and visible platform trials was quantified as latency to the platform in seconds.

### Assessment of brain edema

Brain edema was assessed by measuring brain water content using the (wet-dry)/wet brain weight method. Brains were removed

at 24 or 48 h after injury and bisected into left and right hemispheres. Each hemisphere was weighed (wet weight), then dried at 99°C for 72 h and dry weights were obtained. Percent brain water content was expressed as (wet-dry weight)/wet weight x 100%.

#### Assessment of contusion and lesion volume

At 48 h (contusion volume,  $n=6$  CCI-CHI 83 g and 6 CCI) or 21 days (lesion volume) after injuries, mice were euthanized, and brains were frozen in nitrogen vapor. The brains were sectioned in the coronal plane (14  $\mu\text{m}$ ) at intervals of 0.5 mm from anterior to posterior end. The sections were mounted on poly-L-lysine-coated slides and stained with hematoxylin (lesion volume) or hematoxylin and eosin (H&E, contusion volume). For lesion volume analysis, area of the uninjured and injured hemisphere was measured on each section using image analysis software (NIS Elements BR 3.0, Tokyo, Japan). The hemispheric volume was obtained by summing area of each section and multiplying it by 0.5. Lesion volume ( $\text{mm}^3$ ) was expressed as difference between the uninjured and injured hemisphere volume. For contusion volume analysis, the area of the contusion demarcated by H&E staining was quantified along with the area of non-contused left hemisphere using image analysis as above.

#### Histochemical detection of acute cellular injury and degeneration

We previously reported no acute cell death in CHI (53 g).<sup>12</sup> To determine whether CHI (83 g) induced acute cellular injury, mice were anesthetized briefly in isoflurane, and propidium iodide (PI; Sigma, St. Louis, MO) was administered via intraperitoneal injection (2  $\mu\text{g/g}$  in 200  $\mu\text{L}$  phosphate buffered saline [PBS]) 1 h before euthanasia at 24, 48, or 72 h after CHI (83 g) ( $n=4$ /time point). For detection of acute cellular injury/degeneration in CCI and sequential injury as well as CHI (83 g), H&E staining was also used ( $n=4$ /timepoint). Mice were euthanized and brains were removed and frozen in nitrogen vapor. Cryostat coronal sections (14  $\mu\text{m}$ ) were cut at 250  $\mu\text{m}$  intervals from anterior to posterior hippocampus and mounted on poly-L-lysine-coated slides. Frozen sections were stained with H&E, mounted with Permount, and photographed (NIS Elements BR 3.0). PI labeling was detected in slides not subjected to H&E by fluorescence microscopy using excitation and emission wavelengths of 568 and 585 nm, respectively.

#### Assessment of injured cell counts

For acute cellular injury and death studies in CHI (83 g) mice, brain regions assessed for cell counts were all  $\times 200$  microscopic fields (1100  $\times$  1100  $\mu\text{m}$ ) in cortex ( $n=6$  fields/hemisphere, 5 sections per mouse), hippocampus (1–4 fields per hemisphere  $\times$  5 sections per mouse), and corpus callosum (3 fields/hemisphere  $\times$  5 sections/mouse). Time points examined were 6 ( $n=6$ ), 24, 48, and 72 h ( $n=4$ /timepoint).

For acute cellular injury studies in right hemispheric brain regions in CHI, sequential injury (CCI-CHI) and CCI mice (6 h,  $n=6$ /group), PI+ or argyrophilic cells (H&E) were assessed in the right (uninjured) cortex (6 fields/section) and hippocampus (1–4 fields/section). Cell count data for each mouse were the average of the total number of  $\times 200$  brain fields counted. All cell count data were performed by investigators blinded to study groups.

#### Assessment of APP

For immunohistochemical detection of amyloid precursor protein (APP), frozen sections were air-dried and fixed in 100% ethanol, washed in PBS (pH 7.4), and blocked in 3% normal goat serum/PBS. Sections were incubated overnight at 4°C with rabbit anti-amyloid precursor protein (1:500, Sigma, St. Louis, MO). The

following day, slides were washed in PBS and reacted with the appropriate Cy3 conjugated secondary antibody (1:300; Jackson ImmunoResearch, West Grove, PA) for 60 min, washed in PBS, and cover-slipped for analysis using excitation/emission spectra of 568/585 nm on a Nikon Eclipse Ti-S fluorescence microscope (Micro Video Instruments; Avon, MA). APP-positive axons were evaluated qualitatively in corpus callosum in left and right hemispheres because that is where staining was most robust (CHI, CCI, CCI-CHI 83 g,  $n=4$ /group).

#### Statistical analyses

Data are mean  $\pm$  standard error of the mean, except for right hemisphere PI+ cell counts (median [range]), which were not normally distributed. Data were analyzed using Sigma Stat 3.0 or Graphpad PRISM V (Graphpad Software Inc., La Jolla, CA). Wire-grip test and MWM results were analyzed using two factor repeated measures analysis of variance (RM ANOVA, group  $\times$  time). Physiological variables, seizures, apnea, LOC, edema, lesion volume, and probe trial data were analyzed by ANOVA or ANOVA on ranks and  $t$  test or rank sum test as appropriate. For all comparisons,  $p < 0.05$  was considered significant.

#### Results

A total of 164 mice were used in survival experiments, of which 5 mice died (Table 1). None of the CHI mice examined (0/10 at 53 g and 0/16 at 83 g weight drop) exhibited skull fracture, contusions, or intraparenchymal hemorrhage. Table 2 shows the incidence of seizures and apnea in injured mice. All mice classified as having seizures had bilateral lower extremity tonic-clonic movements and tail stiffening. All seizures lasted less than 60 sec and were only observed immediately after injury during LOC time, and never in awake animals after injury. The incidence of seizures or apnea did not differ between CHI 53 g and 83 g in CHI alone or CCI-CHI.

Baseline physiological variables for CCI and CHI have been published previously by us.<sup>12,15</sup> At 1 and 5 min after sequential injury (CHI 83g-CCI), mice were not acidotic (pH 7.36  $\pm$  0 at 1 min, 7.39  $\pm$  0.1 at 5 min), hypercarbic (PaCO<sub>2</sub> 36  $\pm$  3 Torr at 1 and 32  $\pm$  3 Torr at 5 min), or hypoxic (PaO<sub>2</sub> 178  $\pm$  21 Torr at 1 and 150  $\pm$  23 Torr at 5 min) after injury. Mean arterial blood pressure was 74  $\pm$  4 mm Hg at 3 min ( $p=0.29$  vs. CHI [53 g] reported by Khuman and associates<sup>12</sup>).

TABLE 1. NUMBERS OF MICE USED IN EXPERIMENTS

	LOC	Edema	Lesion volume	Motor	MWM
53 g					
CHI sham	<b>6*</b>			6	6
CCI sham	<b>6</b>		6	6	6
CHI only	<b>10</b>			10	10
CCI only	<b>10</b>	<b>6</b>	10	10	10
CCI-CHI	<b>20</b>		9	9	9
CHI-CCI	<b>16</b>	<b>6</b>	10	10	10
83 g					
CHI sham	<b>6</b>	<b>6</b>	6	6	6
CCI sham	<b>6</b>		6	6	6
CHI only	<b>16</b>	<b>6</b>	16	16	16
CCI only	<b>16</b>	<b>6</b>	15	15	15
CCI-CHI	<b>16</b>		13	14	13
CHI-CCI		<b>6</b>			

\*Numbers in bold indicate those used in calculating total number of mice used in study.

LOC, loss of consciousness; MWM, Morris Water Maze; CHI, closed head injury; CCI, controlled cortical impact.

TABLE 2. INCIDENCE OF SEIZURES AND APNEA

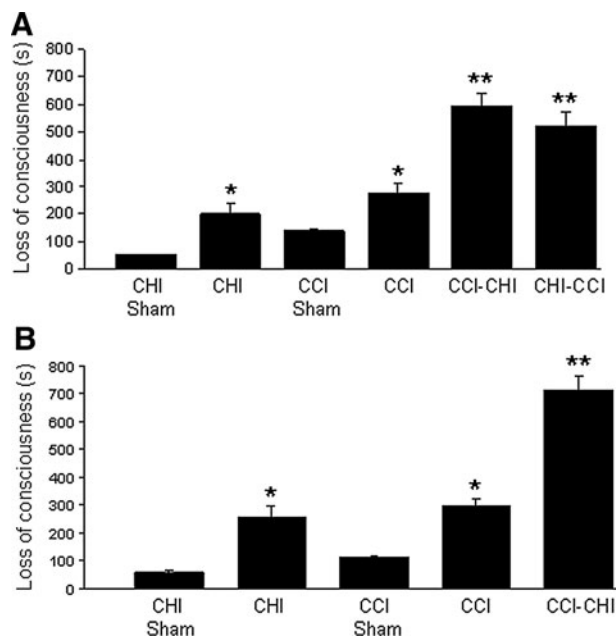
	Seizures			Apnea		
	53 g	83 g	p value*	53 g	83 g	p value*
CHI alone	5/10	12/16	0.31	1/10	4/16	0.55
CCI-CHI	2/20	4/16	0.42	0/20	0/16	1
CHI-CCI	6/18	NA		4/18	NA	

\*Man-Whitney U test (rank sum).

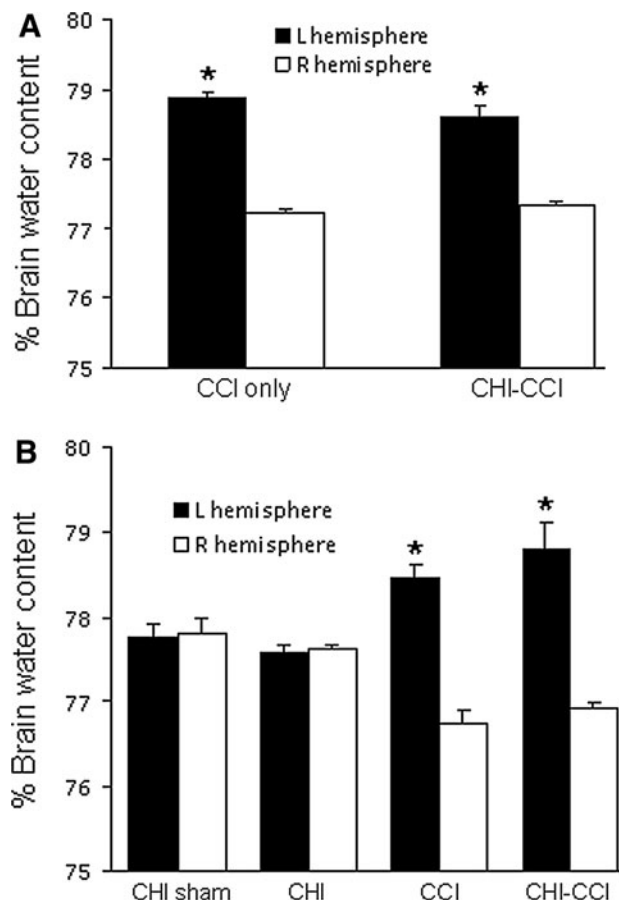
CHI, closed head injury; CCI, controlled cortical impact.

Figure 1A shows LOC times in mice subjected to single and sequential injury using CHI (53 g). As expected, CHI (53 g) and CCI alone produced significantly more LOC compared with their respective sham-injured groups ( $p \leq 0.01$  for both comparisons). Sequential injury groups also had increased LOC times versus single injury groups ( $p < 0.001$  for all comparisons), suggesting an additive effect on LOC. CCI-CHI (53 g), however, did not differ from CHI (53 g)-CCI with respect to LOC ( $p = 0.27$ ). Similar to the findings with CHI (53 g), CCI-CHI (83 g) mice had increased LOC times compared with CCI and CHI (83 g) alone (Fig. 1B).

Figure 2 shows the effect of mixed CHI-CCI on post-injury brain edema assessed 48 h after injury. CCI and CHI-CCI (53 g) induced significant increases in brain water content in injured hemispheres, but brain edema in CHI (53 g)-CCI was similar to that of CCI alone (Fig. 2A). Brain water content in injured hemispheres was also increased to a similar extent between CCI and CHI (83 g)-CCI groups (Fig. 2B).



**FIG. 1.** Loss of consciousness time after single and sequential injury with 53 g closed head injury (CHI). (A) Controlled cortical impact (CCI) and closed head injury (CHI) 53 g each produced significant loss of consciousness (LOC) compared with their respective sham-injured groups ( $p \leq 0.01$  for both comparisons). Sequential injury groups also had increased LOC versus single injury groups (\*\* $p < 0.01$  vs. CCI or CHI). No significant difference in LOC was observed between CCI-CHI versus CHI-CCI ( $p = 0.27$ ). (B) Similar results were obtained after single and sequential injury with 83 g CHI (\*\* $p < 0.01$  for CHI-CCI vs. CCI or CHI).



**FIG. 2.** Brain edema after single and sequential controlled cortical impact (CCI) and closed head injury (CHI). (A) Both CCI and CCI-CHI (53 g) induced significant increases in brain water content in injured hemispheres at 48 h (\* $p < 0.01$  vs. right hemisphere for both groups). Increased brain water content produced by sequential CCI-CHI (53 g) was similar to that produced by CCI alone. (B) Increased brain water content produced by sequential CCI-CHI (83 g) was similar to that produced by CCI alone (\* $p < 0.01$  vs. right hemisphere for both groups).

Figure 3 shows effects of sequential injuries on post-injury lesion volume. Lesion size was greater in CCI versus sham CCI groups ( $p < 0.0001$ ), and was greater in CCI-CHI (53 g) and CHI (53 g)-CCI compared with CCI alone ( $p < 0.05$ , Fig. 3A). Lesion size in CCI-CHI (53 g) did not differ from that of CHI (53 g)-CCI ( $p = 0.25$ ). Post-injury lesion size was also greater in CCI-CHI (83 g) compared with CCI alone, but lesion size did not differ between CCI-CHI (53 g) and CCI-CHI (83 g),  $p = 0.55$  (Fig. 3B).

Figure 4 shows the effect of sequential injuries on post-injury motor function. Compared with sham-injured mice (Fig. 4A), CCI, CCI-CHI (53 g), and CHI (53 g)-CCI produced deficits in the wire-grip test; however, motor deficits after CCI-CHI (53 g) did not differ from those observed after CHI (53 g)-CCI, and neither sequential injury group with CHI 53 g had motor deficits greater than CCI alone (Fig. 4B). CCI-CHI (83 g), however, had greater motor deficits than CHI (83 g) or CCI alone, demonstrating an additive effect of CHI (83 g) to that of CCI (Fig. 4C).

Figure 5 shows results of Morris water maze testing. No differences in hidden or visible platform testing were observed between sham-injured CCI and sham-injured CHI mice (Fig. 5A).

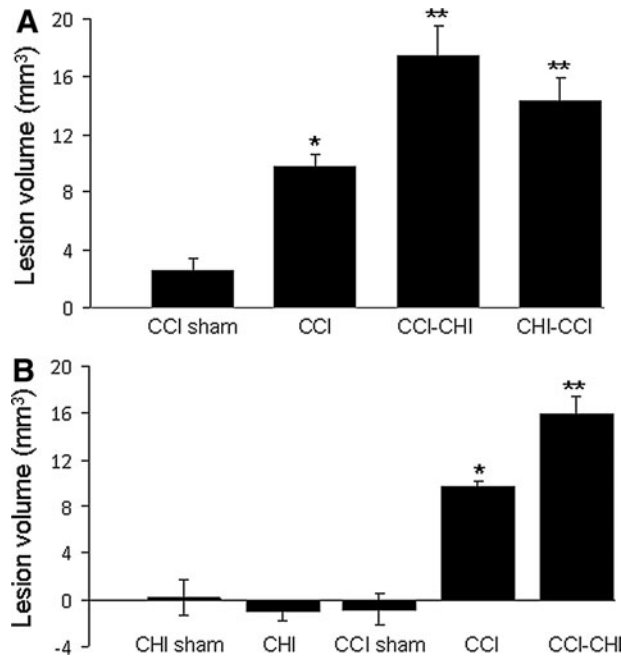
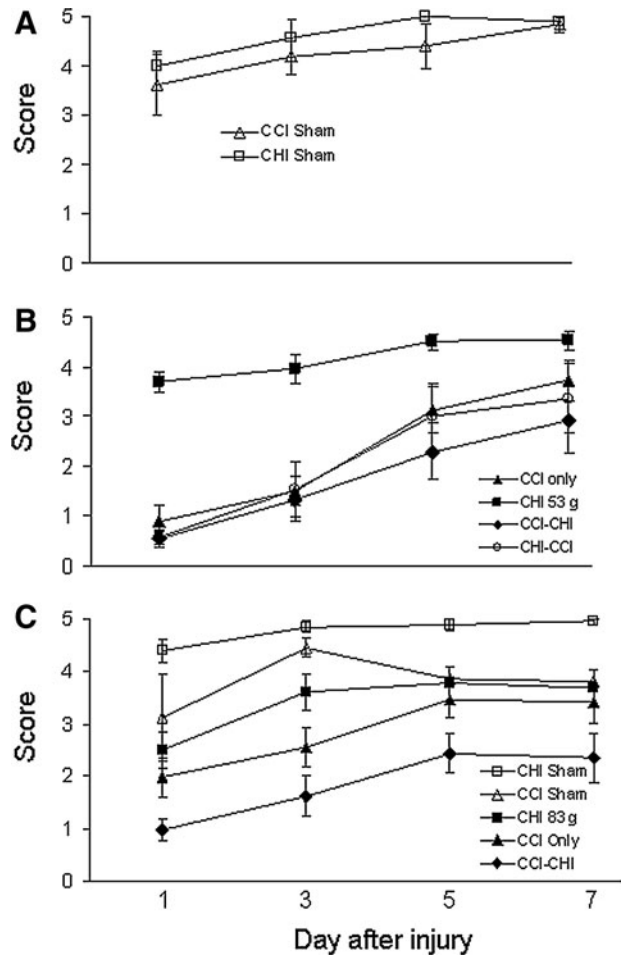


**FIG. 3.** Lesion volume after single and sequential controlled cortical impact (CCI) and closed head injury (CHI). (A) Post-injury lesion size was greater in CCI versus sham CCI groups ( $p < 0.0001$ ) and was greater in CCI-CHI (53 g) and CHI (53 g)-CCI compared with CCI alone ( $p < 0.05$ ). Lesion size in CCI-CHI (53 g) did not differ from that of CHI (53g)-CCI ( $p = 0.25$ ). \* $p < 0.0001$  and \*\* $p < 0.05$  (B) Similar to results with CHI (53 g), lesion volume after injury was significantly greater in CCI-CHI (83 g) compared with CCI alone ( $p < 0.001$ ) but did not differ from that of CCI-CHI (53 g) ( $p = 0.55$ ). \*\* $p < 0.001$  vs. CCI and \* $p < 0.0001$  vs. sham CCI.

Compared with sham-injured mice, CCI but not CHI (53 g) alone produced hidden platform deficits (Fig. 5B). Hidden platform deficits in CCI alone and in both sequential models using 53 g CHI were greater than those observed in CHI (53 g) alone ( $p < 0.05$  for group, hidden platform trials), but no differences were observed among CCI-CHI (53 g), CHI (53 g)-CCI, and CCI groups (Fig. 5B). Likewise, no differences in visible platform ( $p > 0.05$  for group) were observed among the four injury groups using CHI 53 g (Fig. 5B). Figure 5C shows MWM data using CHI (83 g). All injured groups had hidden platform deficits compared with sham-injured CHI and CCI mice. In addition, hidden platform deficits were worse in CCI-CHI (83 g) mice compared with CCI alone ( $p < 0.005$  for group).

Figure 6 shows probe trial data for MWM experiments. Compared with sham-injured mice, all four injury groups (CCI, CHI [53 g], CCI-CHI [53 g], and CHI [53 g]-CCI) had probe trial deficits ( $p < 0.001$  ANOVA,  $p < 0.05$  for each group vs. shams; Fig. 6A). No difference in probe trial performance, however, was observed among the four injury groups using 53 g ( $p = 0.3$  ANOVA). Compared with sham-injured (CHI or CCI) mice, probe trial deficits were also observed in CCI, CCI-CHI (83 g), and CHI (83 g) mice (Fig. 6B).

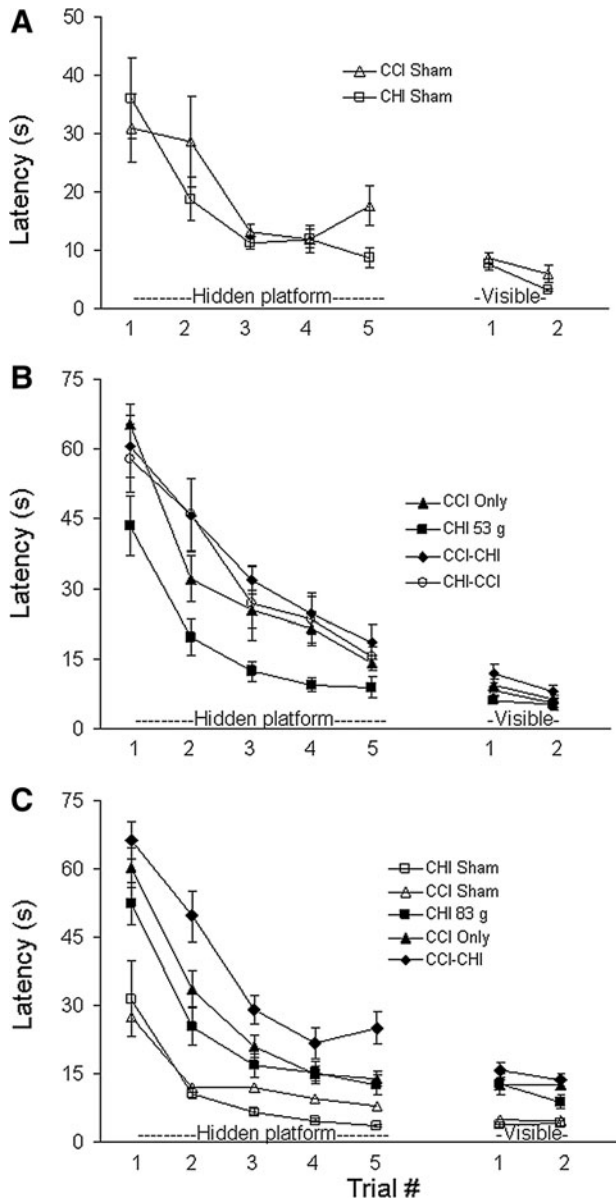
Figure 7 shows gross histopathology of sequential injury (CCI-CHI 83 g) compared with CCI and CHI (83 g). At 2 weeks after injury, a cavitory lesion involving damage to cortex and underlying hippocampus was observed in all CCI and sequential injury mice, with overall lesion size greater in sequential injury (Fig. 7A, Fig. 3). Representative photomicrographs of extent of contusion in CCI and



**FIG. 4.** Motor performance after single and sequential controlled cortical impact (CCI) and closed head injury (CHI). (A) No difference in wire-grip test performance was observed between sham-injured CCI and CHI mice. (B) Compared with sham-injured mice and to CHI (53 g) alone, CCI, CCI-CHI (53 g), and CHI (53 g)-CCI produced deficits in the wire-grip test ( $p < 0.005$  for group for each comparison to sham or CHI [53 g]). Neither CCI-CHI (53 g) nor CHI (53 g)-CCI, however, had motor deficits greater than CCI alone, and CCI-CHI (53 g) performed similarly to CHI (53 g)-CCI. (C) Motor deficits after CCI-CHI (83 g) were significantly greater than CHI (83 g) or CCI alone ( $p < 0.05$  for group).

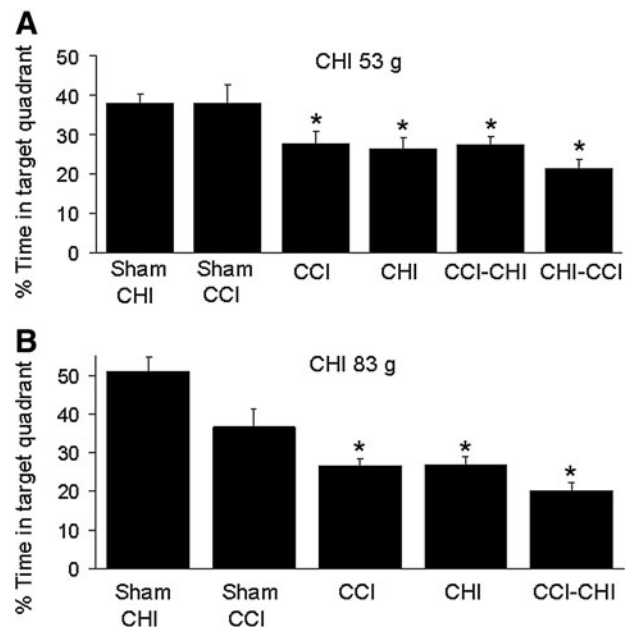
sequential injury mice (48 h) are shown in Figure 7B. Quantitative analysis showed that contusion volume was similar between groups (CCI,  $26 \pm 4.6$ ; sequential,  $24.3 \pm 2.7$  mm<sup>3</sup>,  $p = 0.74$ ,  $n = 6$ /group). Likewise, non-contused left hemispheric volume was also similar between CCI ( $98.3 \pm 5.4$  mm<sup>3</sup>) and sequential injury ( $89.6 \pm 4.0$  mm<sup>3</sup>) ( $p = 0.2$ ), consistent with brain edema data (Fig. 2).

Figure 8 shows histopathology of acute cellular and axonal injury in CHI (83 g), CCI, and sequential injury (CCI-CHI 83 g) mice. In CHI (83 g), no PI+ or argyrophilic (H&E) cells were observed in  $\times 200$  fields in injured cortices, hippocampi, or corpus callosum at 24, 48, or 72 h in any of the mice examined ( $n = 4$ /time point). As expected, mice subjected to CCI and sequential injury had large numbers of degenerative cells in the left hemispheric cortex and hippocampus at 6 h (not shown). Degenerative cells were not detected in right hemispheric brain regions of CCI or CHI mice, but were significantly increased in right hemispheric dentate gyrus



**FIG. 5.** Morris water maze performance after single and sequential controlled cortical impact (CCI) and closed head injury (CHI). (A) Sham-injured CCI and CHI groups did not differ with respect to performance in hidden and visible platform trials. (B) CCI ( $p < 0.05$  for group) but not CHI (53 g) alone produced hidden platform deficits compared with shams. Hidden platform deficits in CCI alone and in both sequential models (CCI-CHI 53 g and CHI 53 g-CCI) were greater than those observed in CHI (53 g) alone ( $p < 0.05$  for group), but no differences were observed among CCI-CHI (53 g), CHI (53 g)-CCI, and CCI groups. Likewise, no differences in visible platform ( $p > 0.05$  for group). (C) CCI-CHI (83 g) mice had hidden platform deficits compared with CCI alone ( $p < 0.005$  for group), indicating an additive effect of CHI (83 g) to that of CCI in the sequential injury group.

(arrow; PI+ cells in inset) of sequential injury mice (CCI-CHI 83 g, 3.5 [82.2]; CCI, 0 [0]; CHI 83g, 0 [0] PI+ cells/ $\times 200$  field;  $p = 0.002$  ANOVA;  $p < 0.05$  CCI-CHI [83 g] vs. CHI 83 g and CCI). No degenerative cells were detected in CA1 or CA3 in sequential injury, CCI, or CHI mice.



**FIG. 6.** Probe trials after single and sequential controlled cortical impact (CCI) and closed head injury (CHI). (A) Compared with sham-injured mice, all four injury groups (CCI, CHI [53 g], CCI-CHI [53 g], and CHI [53 g]-CCI) had probe trial deficits ( $p < 0.001$  analysis of variance [ANOVA],  $p < 0.05$  for each group vs. combined sham CHI and sham CCI mice). No differences in probe trial deficits ( $p = 0.3$  ANOVA) were observed among the four CHI (53 g) injury groups. (B) Using CHI (83 g), all three injury groups had probe trial deficits compared with sham-injured mice ( $p < 0.01$  ANOVA;  $*p < 0.05$  vs. sham-injured) but no differences were detected among injury groups.

With respect to axon injury, APP staining was robustly detected at 6 h in injured cortex and corpus callosum of CCI-CHI 83 g and CCI mice, whereas APP was only occasionally detected in corpus callosum of CHI (83 g) mice (Fig. 8B). In right hemispheric hippocampal fields, APP-positive axons were only occasionally observed and did not appear to differ among CCI, CHI, and CHI-CCI mice at 6 or 48 h. Scale bars = 100  $\mu$ m.

**Discussion**

Using a novel sequential concussive and contusion brain injury model in mice, we found that combination TBI produced additive effects in LOC and post-injury lesion volume compared with either CCI or CHI (53 or 83 g). Post-injury motor and Morris water maze deficits in the (53 g) sequential model were similar to those observed in CCI alone, whereas a higher CHI level (83 g weight drop) produced additional motor and cognitive deficits in sequential injury compared with CCI alone. Additive effects in gross histopathology and LOC time were observed regardless of the order of injury (CHI-CCI vs. CCI-CHI), and increased right dentate gyrus cell death was produced by sequential injury versus CCI and CHI (83 g). The data suggest an interaction between concussive and contusion brain injury that leads to worse histopathological and functional outcome in a CHI dose-dependent manner.

Regardless of the order in which injuries (CCI or CHI) were performed, we found additive effects in sequential injury models (53 g CHI) with respect to LOC and lesion volume. Interestingly, 83 g CHI did not increase lesion size beyond that of 53 g CHI in

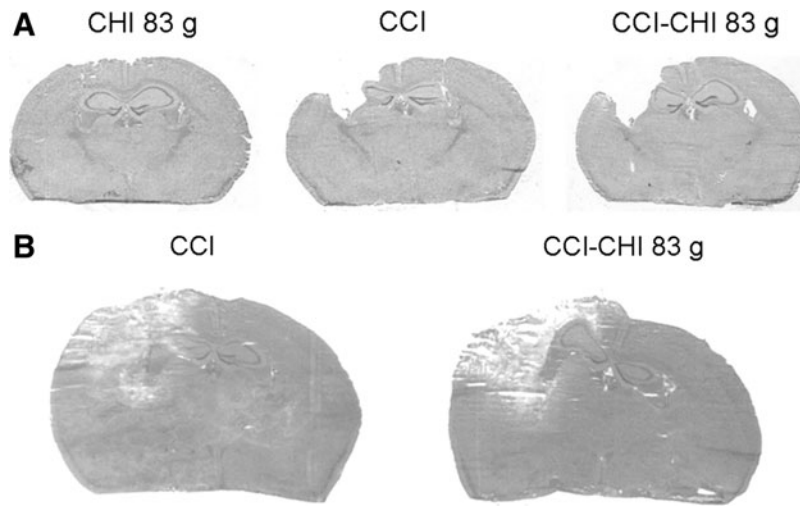


**FIG. 7.** Gross histopathology of single and sequential controlled cortical impact (CCI) and closed head injury (CHI). Representative photomicrographs of hematoxylin and eosin-stained brain sections depicting (A) lesion volume (21 days) and (B) extent of contusion (48 h) in injured mice.

sequential injury models, suggesting a possible ceiling effect of CHI between 53 and 83 g (Fig. 3). The data suggest that the latency between injuries (approximately 1–2 min) is not a factor that significantly influences the interaction between concussion and contusion in the sequential TBI models. Nonetheless, because our model features sequential and not concomitantly produced injuries, we cannot claim that the sequential injury model reported here precisely models the clinical scenario in which concussion and contusion occur simultaneously in patients with TBI.

In our previous report, CHI (53 g) produced over the center of the head led to hidden platform as well as probe trial deficits in the Morris water maze.<sup>12</sup> The modified CHI used in the current study, however, in which the head was impacted above the right ear (to avoid striking contused brain in CCI-CHI), failed to produce deficits in hidden platform trials in CHI (53 g). This is likely explained by a less severe brain injury, because this modification also reduced mortality rate from approximately 20% to 0/10 (CHI 53 g) and 0/16 (CHI 83 g) in the current study and reduced the incidence of

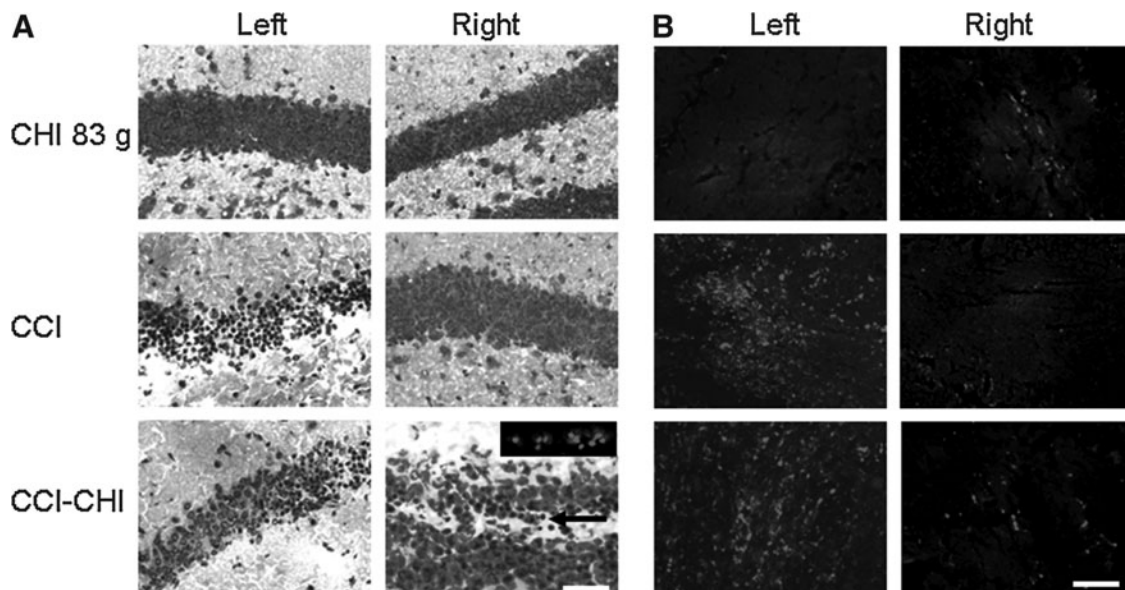


**FIG. 8.** Microscopic histopathology of single and sequential controlled cortical impact (CCI) and closed head injury (CHI). (A) Representative photomicrographs of hematoxylin and eosin staining at 6 h after CHI, CCI, or CCI-CHI showing acute cellular injury (argyrophilic cells) in left hemispheric hippocampus of CCI and CCI-CHI mice but not CHI. In contrast, no acute cellular injury/death was observed in right hemispheric hippocampus (dentate gyrus shown in all micrographs) of CCI or CHI, but degenerative cells were noted in right dentate gyrus of sequential injury mice. Inset, representative example of propidium iodide labeling of right sided dentate gyrus cells 6 h after CCI-CHI 83 g. (B) Amyloid precursor protein (APP) immunohistochemistry showing robust axonal injury in left hemispheric corpus callosum after CCI and CCI-CHI but not CHI. Only occasional APP-positive axons were detected in right hemispheres in each group. Scale bar, 100  $\mu$ m.

seizures by 50% (53 g CHI) as well.<sup>12</sup> Because the modified CHI model behaved differently in the current study, we characterized it in terms of LOC, edema, lesion volume, histopathology, and motor and cognitive deficits so that valid conclusions could be drawn from the sequential injury model data here.

Sequential injury (using either 53 or 83 g CHI) induced additive LOC versus CHI and CCI alone. Increased LOC in the sequential model was not an artifact of the anesthesia regimen, because mice subjected to sequential injury were exposed to similar depth and duration of anesthesia as mice subjected to CCI alone. There are very few studies examining mechanisms of LOC in rodent TBI models; however, posttraumatic coma has been associated with degree of axonal injury in rodent and human TBI.<sup>18,19</sup> Axonal injury is a prominent feature of CCI<sup>20</sup> but is infrequently detected in the CHI model by APP immunohistochemistry (current study) or by electron microscopy.<sup>12</sup> LOC was significantly increased in a sequential linear/angular acceleration model compared with linear or angular acceleration alone, and sequential injury also significantly increased axonal damage in that study.<sup>19</sup>

We found a decreased incidence of seizure activity in sequential injury (CCI-CHI) mice compared with mice subjected to CHI alone. This observation suggests that CCI somehow reduces seizure vulnerability to CHI. Cortical spreading depression produced immediately after CCI is associated with profound reduction in electroencephalographic activity to less than 15% of baseline; this effect lasts several minutes before slowly recovering and may be one reason why seizure activity is reduced when CHI follows CCI.<sup>21</sup>

Focal (CCI) and concussive (CHI) mechanisms may each contribute to outcome in severely injured patients whose TBI is characterized by more than one injury type secondary to focal and inertial loading mechanisms.<sup>1,22</sup> Inasmuch as sequential injury produced additive effects on histopathological and functional outcome, our study is in principle similar to other injury models in which TBI was combined with controlled secondary insults to mimic the clinical scenarios of superimposed hypoxemia,<sup>23,24</sup> systemic hemorrhage,<sup>25</sup> polytrauma,<sup>26</sup> and seizures.<sup>27</sup>

Others have also reported TBI consisting of simultaneous linear and angular head acceleration.<sup>28,19</sup> In the model by Marmarou and colleagues,<sup>29</sup> combined impact and linear acceleration produces robust diffuse axonal injury but not contusion. Sequential injury reported herein differs from that of the Marmarou model because sequential injury produces cerebral contusion with relatively little axonal injury (detected by APP histochemistry). Interestingly, sequential injury produced a significant, albeit modest, increase in cell death in the right hemispheric dentate gyrus versus CCI and CHI alone. Whether CHI exacerbates histopathology of CCI or *vice versa* is not discernable from the current study design; however, the present data suggest an interaction between CCI and CHI that produces increased cell death even in the intact right hemisphere, which may contribute to the observed exacerbation of cognitive deficits in the CCI-CHI (83 g) model. One caveat is that APP histochemistry is not as sensitive as silver staining for detecting cell and axonal damage; thus, more work is needed to fully characterize the histopathology of sequential injury.

The current study is unique and fills a gap in the literature by using concussive and contusion injury mechanisms in a sequential TBI model.

How CHI (which does not result in acute brain cell death/tissue loss<sup>12</sup>; Fig. 3) increases brain tissue damage in sequential CHI-CCI is unknown. Physiological variables obtained at 1–2 min after CCI-CHI (83 g) suggest that hypotension and hypoxemia, known to worsen outcome after TBI,<sup>30</sup> do not play a major role. Mechanisms

associated with concussive injury (reviewed by Barkhoudarian and coworkers<sup>31</sup>) that could explain the increased tissue damage in the sequential model might include excitotoxicity and calcium and other ion fluxes,<sup>32</sup> hyperglycolysis and mitochondrial energy failure,<sup>33–35</sup> loss of cerebral blood flow autoregulation,<sup>36</sup> and changes in cortical spreading depression, although a recent study suggests that this mechanism may not be critical for contusion TBI.<sup>21</sup>

Molecular mechanisms that may be exacerbated by sequential injury include deranged electron transport and oxidative stress, apoptosis and necrosis. Increased inflammation may be particularly damaging because it may increase the volume of ischemic brain tissue in the contusion core *via* microvascular plugging,<sup>37,38</sup> or by exacerbating acute cell death. We previously reported that CHI renders the injured brain more vulnerable to cytokines that initiate programmed cell death acutely after CCI<sup>5,12</sup>; however, we did not observe increased contusion volume at 48 h in sequential injury versus CCI, suggesting that the increased lesion volume at 14 days after sequential injury may be because of increased brain tissue atrophy rather than increases in contusion size and acute cell death. Alternatively, concussive forces might exacerbate brain tissue loss after focal injury by increasing delayed (e.g., up to 14 days) inflammation, leading to neurodegeneration induced by activated microglia and/or astrocytes.<sup>39–42</sup> Distinguishing between these and other explanations for why concussive forces might exacerbate brain tissue damage after cerebral contusion is an important direction for future studies.

Modeling two different TBI injury subtypes is important for at least two reasons. First, the failure of all randomized clinical trials except one<sup>43</sup> to show a positive effect of treatment strategies on outcome after TBI may relate in part to oversimplified TBI models that fail to account for the heterogeneity of injury mechanisms in severely injured patients. In this regard, the same molecular pathway in one injury subtype may behave differently in another, complicating targeted therapeutic strategies.<sup>5,12</sup> One goal of future studies is to examine the role of key pathways (known to mediate outcome in CCI and CHI) in the sequential injury model. Such studies have the potential to improve understanding of how specific mechanisms might contribute to outcome in severely injured patients with mixed injury types.

The second reason to study sequential injury models is related to the first: it is possible that therapies that work in a more complex sequential TBI model might translate better in human trials that enroll patients with mixed injury subtypes. Future studies in our laboratory will seek to identify therapies that reduce histopathology and improve functional outcome after sequential CCI-CHI. It is hoped that positive effects in this more complex TBI model might have an increased chance of translating to human studies.

## Acknowledgments

We thank Michael A. Moskowitz, M.D. for help with arterial blood gas and blood pressure measurements.

This work was supported by 1R21NS075226, RO1NS047447 and RO1NS064545 (MJW).

## Author Disclosure Statement

No competing financial interests exist.

## References

1. Saatman, K.E., Duhaime, A.C., Bullock, R., Maas, A.I., Valadka, A., and Manley, G.T. (2008). Classification of traumatic brain injury for targeted therapies. *J. Neurotrauma* 25, 719–738.



2. Yoganandan, N., Gennarelli, T.A., Zhang, J., Pintar, F.A., Takhounts, E., and Ridella, S.A. (2009). Association of contact loading in diffuse axonal injuries from motor vehicle crashes. *J. Trauma* 66, 309–315.
3. Narayan, R.K., Michel, M.E., Ansell, B., Baethmann, A., Biegon, A., Bracken, M.B., Bullock, M.R., Choi, S.C., Clifton, G.L., Contant, C.F., Coplin, W.M., Dietrich, W.D., Ghajar, J., Grady, S.M., Grossman, R.G., Hall, E.D., Heetderks, W., Hovda, D.A., Jallo, J., Katz, R.L., Knoller, N., Kochanek, P.M., Maas, A.I., Majde, J., Marion, D.W., Marmarou, A., Marshall, L.F., McIntosh, T.K., Miller, E., Mohberg, N., Muizelaar, J.P., Pitts, L.H., Quinn, P., Riesenfeld, G., Robertson, C.S., Strauss, K.I., Teasdale, G., Temkin, N., Tuma, R., Wade, C., Walker, M.D., Weinrich, M., Whyte, J., Wilberger, J., Young, A.B., and Yurkewicz, L. (2002). Clinical trials in head injury. *J. Neurotrauma* 19, 503–557.
4. Bempohl, D., You, Z., Korsmeyer, S.J., Moskowitz, M.A., and Whalen, M.J. (2006). Traumatic brain injury in mice deficient in Bid: effects on histopathology and functional outcome. *J. Cereb. Blood Flow Metab.* 26, 625–633.
5. Bempohl, D., You, Z., Lo, E.H., Kim, H.H., and Whalen, M.J. (2007). TNF alpha and Fas mediate tissue damage and functional outcome after traumatic brain injury in mice. *J. Cereb. Blood Flow Metab.* 27, 1806–1818.
6. Sinz, E.H., Kochanek, P.M., Dixon, C.E., Clark, R.S., Carcillo, J.A., Schiding, J.K., Chen, M., Wisniewski, S.R., Carlos, T.M., Williams, D., DeKosky, S.T., Watkins, S.C., Marion, D.W., and Billiar, T.R. (1999). Inducible nitric oxide synthase is an endogenous neuroprotectant after traumatic brain injury in rats and mice. *J. Clin. Invest.* 104, 647–656.
7. Smith, D.H., Soares, H.D., Pierce, J.S., Perlman, K.G., Saatman, K.E., Meaney, D.F., Dixon, C.E., and McIntosh, T.K. (1995). A model of parasagittal controlled cortical impact in the mouse: cognitive and histopathologic effects. *J. Neurotrauma* 12, 169–178.
8. Whalen, M.J., Carlos, T.M., Dixon, C.E., Schiding, J.K., Clark, R.S., Baum, E., Yan, H.Q., Marion, D.W., and Kochanek, P.M. (1999). Effect of traumatic brain injury in mice deficient in intercellular adhesion molecule-1: assessment of histopathologic and functional outcome. *J. Neurotrauma* 16, 299–309.
9. McCrory, P., Meeuwisse, W., Johnston, K., Dvorak, J., Aubry, M., Molloy, M., and Cantu R. (2009). Consensus statement on Concussion in Sport—the 3rd International Conference on Concussion in Sport held in Zurich, November 2008. *J. Sci. Med. Sport* 12, 340–351.
10. Ommaya, A.K., and Gennarelli, T.A. (1974). Cerebral concussion and traumatic unconsciousness. Correlation of experimental and clinical observations of blunt head injuries. *Brain* 97, 633–654.
11. Viano, D.C., Casson, I.R., and Pellman, E.J. (2007). Concussion in professional football: biomechanics of the struck player—part 14. *Neurosurgery* 61, 313–328.
12. Khuman, J., Meehan, W.P., 3rd, Zhu, X., Qiu, J., Hoffmann, U., Zhang, J., Giovannone, E., Lo, E.H., and Whalen, M.J. (2011). Tumor necrosis factor alpha and Fas receptor contribute to cognitive deficits independent of cell death after concussive traumatic brain injury in mice. *J. Cereb. Blood Flow Metab.* 31, 778–789.
13. Khuman, J., Zhang, J., Park, J., Carroll, J.D., Donahue, C., and Whalen, M.J. (2012). Low-level laser light therapy improves cognitive deficits and inhibits microglial activation after controlled cortical impact in mice. *J. Neurotrauma* 29, 408–417.
14. Yager, P.H., You, Z., Qin, T., Kim, H.H., Takahashi, K., Ezekowitz, A.B., Stahl, G.L., Carroll, M.C., and Whalen, M.J. (2008). Mannose binding lectin gene deficiency increases susceptibility to traumatic brain injury in mice. *J. Cereb. Blood Flow Metab.* 28, 1030–1039.
15. Yang, J., You, Z., Kim, H.H., Hwang, S.K., Khuman, J., Guo, S., Lo, E.H., and Whalen, M.J. (2010). Genetic analysis of the role of tumor necrosis factor receptors in functional outcome after traumatic brain injury in mice. *J. Neurotrauma* 27, 1037–1046.
16. Racine, R.J. (1972). Modification of seizure activity by electrical stimulation. II. Motor seizure. *Electroencephalogr. Clin. Neurophysiol.* 32, 281–294.
17. Golarai, G., Greenwood, A.C., Feeney, D.M., and Connor, J.A. (2001). Physiological and structural evidence for hippocampal involvement in persistent seizure susceptibility after traumatic brain injury. *J. Neurosci.* 21, 8523–8537.
18. Jenkins, A., Teasdale, G., Hadley, M.D., Macpherson, P., and Rowan, J.O. (1986). Brain lesions detected by magnetic resonance imaging in mild and severe head injuries. *Lancet* 2, 445–446.
19. Wang, H.C., Duan, Z.X., Wu, F.F., Xie, L., Zhang, H., and Ma, Y.B. (2010). A new rat model for diffuse axonal injury using a combination of linear acceleration and angular acceleration. *J. Neurotrauma* 27, 707–719.
20. Meaney, D.F., Ros, D.T., Winkelstein, B.A., Brasko, J., Goldstein, D., Bilston, L.B., Thibault, L.E., and Gennarelli, T.A. (1994). Modification of the cortical impact model to produce axonal injury in the rat cerebral cortex. *J. Neurotrauma* 11, 599–612.
21. von Baumgarten, L., Trabold, R., Thal, S., Back, T., and Plesnila, N. (2008). Role of cortical spreading depressions for secondary brain damage after traumatic brain injury in mice. *J. Cereb. Blood Flow Metab.* 28, 1353–1360.
22. Adams, J.H., Graham, D.I., Murray, L.S., and Scott, G. (1982). Diffuse axonal injury due to nonmissile head injury in humans: an analysis of 45 cases. *Ann. Neurol.* 12, 557–563.
23. Clark, R.S., Kochanek, P.M., Dixon, C.E., Chen, M., Marion, D.W., Heineman, S., DeKosky, S.T., and Graham, S.H. (1997). Early neuropathologic effects of mild or moderate hypoxemia after controlled cortical impact injury in rats. *J. Neurotrauma* 14, 179–189.
24. Feng, J.F., Zhao, X., Gurkoff, G.G., Van, K.C., Shahlaie, K., and Lyeth, B.G. (2012). Post-traumatic hypoxia exacerbates neuronal cell death in the hippocampus. *J. Neurotrauma* 29, 1167–1179.
25. Shellington, D.K., Du, L., Wu, X., Exo, J., Vagni, V., Ma, L., Janesko-Feldman, K., Clark, R.S., Bayir, H., Dixon, C.E., Jenkins, L.W., Hsia, C.J., and Kochanek, P.M. (2011). Polynitroxylated pegylated hemoglobin: a novel neuroprotective hemoglobin for acute volume-limited fluid resuscitation after combined traumatic brain injury and hemorrhagic hypotension in mice. *Crit. Care Med.* 39, 494–505.
26. Mirzayan, M.J., Probst, C., Samii, M., Krettek, C., Gharabaghi, A., Pape, H.C., van Griensven, M., and Samii, A. (2012). Histopathological features of the brain, liver, kidney and spleen following an innovative polytrauma model of the mouse. *Exp. Toxicol. Pathol.* 64, 133–139.
27. Chrzasczcz, M., Venkatesan, C., Dragisic, T., Watterson, D.M., and Wainwright, M.S. (2010). Minoxidil treatment prevents increased seizure susceptibility in a mouse “two-hit” model of closed skull traumatic brain injury and electroconvulsive shock-induced seizures. *J. Neurotrauma* 27, 1283–1295.
28. Li, X.Y., Li, J., Feng, D.F., and Gu, L. (2010). Diffuse axonal injury induced by simultaneous moderate linear and angular head accelerations in rats. *Neuroscience* 169:357–369.
29. Marmarou, A., Foda, M.A., van den Brink, W., Campbell, J., Kita, H., and Demetriadou, K. (1994). A new model of diffuse brain injury in rats. Part I: Pathophysiology and biomechanics. *J. Neurosurg.* 80, 291–300.
30. Bratton, S.L., Chestnut, R.M., Ghajar, J., McConnell Hammond, F.F., Harris, O.A., Hartl, R., Manley, G.T., Nemecek, A., Newell, D.W., Rosenthal, G., Schouten, J., Shutter, L., Timmons, S.D., Ullman, J.S., Videtta, W., Wilberger, J.E., and Wright, D.W. (2007). Guidelines for the management of severe traumatic brain injury. I. Blood pressure and oxygenation. *J. Neurotrauma* 24, Suppl 1, S7–S13.
31. Barkhoudarian, G., Hovda, D.A., and Giza, C.C. (2011). The molecular pathophysiology of concussive brain injury. *Clin. Sports Med.* 30, 33–38.
32. Katayama, Y., Becker, D.P., Tamura, T., and Hovda, D.A. (1990). Massive increases in extracellular potassium and the indiscriminate release of glutamate following concussive brain injury. *J. Neurosurg.* 73, 889–900.
33. Yoshino, A., Hovda, D.A., Kawamata, T., Katayama, Y., and Becker, D.P. (1991). Dynamic changes in local cerebral glucose utilization following cerebral concussion in rats: evidence of a hyper and subsequent hypometabolic state. *Brain Res.* 561, 106–119.
34. Xiong, Y., Gu, Q., Peterson, P.L., Muizelaar, J.P., and Lee, C.P. (1997). Mitochondrial dysfunction and calcium perturbation induced by traumatic brain injury. *J. Neurotrauma* 14, 23–34.
35. Perez-Pinzon, M., Stetler, R.A., and Fiskum, G. (2012). Novel mitochondrial targets for neuroprotection. *J. Cereb. Blood Flow Metab.* 32, 1362–1376.
36. Martin, N.A., Patwardhan, R.V., Alexander, M.J., Africk, C.Z., Lee, J.H., Shalmon, E., Hovda, D.A., and Becker, D.P. (1997). Characterization of cerebral hemodynamic phases following severe head trauma: hypoperfusion, hyperemia, and vasospasm. *J. Neurosurg.* 87, 9–19.
37. Engel, D.C., Mies, G., Terpolilli, N.A., Trabold, R., Loch, A., De Zeeuw, C.I., Weber, J.T., Maas, A.I., and Plesnila, N. (2008). Changes

- of cerebral blood flow during the secondary expansion of a cortical contusion assessed by <sup>14</sup>C-iodoantipyrine autoradiography in mice using a non-invasive protocol. *J. Neurotrauma* 25, 739–753.
38. Schwarzmaier, S.M., Kim, S.W., Trabold, R., and Plesnila, N. (2010). Temporal profile of thrombogenesis in the cerebral microcirculation after traumatic brain injury in mice. *J. Neurotrauma* 27, 121–130.
  39. Byrnes, K.R., Loane, D.J., Stoica, B.A., Zhang, J., and Faden, A.I. (2012). Delayed mGluR5 activation limits neuroinflammation and neurodegeneration after traumatic brain injury. *J. Neuroinflammation* 9, 43.
  40. Faden, A.I. (2011). Microglial activation and traumatic brain injury. *Ann. Neurol.* 70, 345–346.
  41. Wang XJ, Zhang S, Yan ZQ, Zhao YX, Zhou HY, Wang Y, Lu GQ and Zhang JD. (2011). Impaired CD200-CD200R-mediated microglia silencing enhances midbrain dopaminergic neurodegeneration: roles of aging, superoxide, NADPH oxidase, and p38 MAPK. *Free Radic. Biol. Med.* 50, 1094–1106.
  42. Zhou, Y., Wang, Y., Kovacs, M., Jin, J., and Zhang, J. (2005). Microglial activation induced by neurodegeneration: a proteomic analysis. *Mol. Cell Proteomics* 4, 1471–1479.
  43. Giacino, J.T., Whyte, J., Bagiella, E., Kalmar, K., Childs, N., Khademi, A., Eifert, B., Long, D., Katz, D.I., Cho, S., Yablon, S.A., Luther, M., Hammond, F.M., Nordenbo, A., Novak, P., Mercer, W., Maurer-Karattup, P., and Sherer, M. (2012). Placebo-controlled trial of amantadine for severe traumatic brain injury. *N. Engl. J. Med.* 366, 819–826.

Address correspondence to:

*Michael J. Whalen, MD*

*Department of Pediatric Critical Care Medicine*

*Massachusetts General Hospital*

*Charlestown, MA 02129*

*E-mail: mwhalen@partners.org*